Plant Physiology, February 1999, Vol. 119, pp. 399–407, www.plantphysiol.org © 1999 American Society of Plant Physiologists

The Site of Oxygen Limitation in Soybean Nodules[1]

Monika M. Kuzma, Heike Winter, Paul Storer, Ivan Oresnik, Craig A. Atkins, and David B. Layzell*

Biology Department, Biosciences Complex, Queen's University, Kingston, Ontario, Canada K7L 3N6 (M.M.K., D.B.L.); Department of Botany, North Carolina State University, Raleigh, North Carolina 27607 (H.W.); Botany Department, University of Western Australia, Nedlands, WA 6907, Australia (P.S., C.A.A.); and Department of Biological Sciences, University of Calgary, Calgary, Alberta, Canada T2N 1N4 (I.O.)

In legume nodules the [O_2] in the infected cells limits respiration and nitrogenase activity, becoming more severe if nodules are exposed to subambient O_2 levels. To identify the site of O_2 limitation, adenylate pools were measured in soybean (*Glycine max*) nodules that were frozen in liquid N_2 before being ground, lyophilized, sonicated, and separated on density gradients of nonaqueous solvents (heptane/tetrachloroethylene) to yield fractions enriched in bacteroid or plant components. In nodules maintained in air, the adenylate energy charge (AEC = [ATP + 0.5 ADP]/[ATP + ADP + AMP]) was lower in the plant compartment (0.65 ± 0.04) than in the bacteroids (0.76 ± 0.095), but did not change when the nodulated root system was exposed to 10% O_2. In contrast, 10% O_2 decreased the bacteroid AEC to 0.56 ± 0.06, leading to the conclusion that they are the primary site of O_2 limitation in nodules. To account for the low but unchanged AEC in the plant compartment and for the evidence that mitochondria are localized in O_2-enriched microenvironments adjacent to intercellular spaces, we propose that steep adenylate gradients may exist between the site of ATP synthesis (and ADP use) in the mitochondria and the extramitochondrial sites of ATP use (and ADP production) throughout the large, infected cells.

Root nodules are the site of a beneficial symbiotic association between legume plants and certain soil bacteria of the *Rhizobium* or *Bradyrhizobium* genera. The plant supplies the bacteria with an energy source (e.g. malate or succinate) and, in turn, the bacteria reduce (fix) the atmospheric N_2 gas to NH_4^+, providing it to the plant for assimilation into amino acids, protein, and other essential nitrogenous compounds. The nitrogenase enzyme responsible for N_2 fixation is O_2 labile, and, presumably to protect nitrogenase from damage, legume nodules have evolved mechanisms to regulate their permeability to O_2 (Hunt et al., 1987; Witty et al., 1987; Hunt and Layzell, 1993). O_2 in the infected cell is maintained at an extremely low concentration (5–50 nM) compared with that in cells in equilibrium with air (approximately 250 μM) (King and Layzell, 1991; Denison et al., 1992; Kuzma et al., 1993). Hunt et al. (1989) have shown that gradual increases in the external partial pressure of O_2 result in small (2%–20%) but significant stimulations in nodule respiration and nitrogenase activity. Moreover, in nodules in which nitrogenase is inhibited due to photosynthate deprivation, nitrate fertilization, or Ar:O_2 exposure, much greater stimulations (50%–300%) in their metabolism can be achieved by increasing the external partial pressure of O_2 (Hartwig et al., 1987; Vessey et al., 1988; Denison et al., 1992; de Lima et al., 1994). Thus, the metabolism of legume nodules is thought to be limited by the O_2 supply at all times; by controlling permeability to O_2 diffusion, nodules are able to reduce further the supply of O_2 to the infected cells and thereby down-regulate metabolism.

For more than 30 years the predominant view has been that in vivo, bacteroids are limited by O_2 availability, presumably by restricting aerobic respiration and thereby ATP supply to nitrogenase (Bergersen, 1962, 1984; Dilworth, 1974; McDermott et al., 1989; Werner, 1992). This view is supported by studies that show a positive correlation between ATP pools and nitrogenase activity in free-living, anaerobically grown diazotrophic bacteria, in isolated bacteroids, or in bacteria induced to fix N_2 under O_2-limiting conditions (Upchurch and Mortenson, 1980; Ching et al., 1981; Privalle and Burris, 1983).

However, the K_m (O_2) for the terminal oxidases of nodule mitochondria (50–100 nM; Rawsthorne and LaRue, 1986; Millar et al., 1995) is greater than that for bacteroids (5–20 nM; Bergersen and Turner, 1993), suggesting that at the low [O_2] in the infected cells (5–50 nM), O_2 would limit mitochondrial respiration rather than bacteroid respiration. However, the mitochondria appear to be localized adjacent to intercellular spaces and therefore may experience higher [O_2] than the bacteria that are found farther away from the spaces (Bergersen, 1994; Thumfort et al., 1994).

A common indicator of hypoxic metabolism in biological systems is the relative size of the adenylate pools. In hypoxic cells the concentration of ATP is typically lower, whereas ADP and AMP pools are higher than those found in aerobic cells (Pradet and Raymond, 1983). Consequently, values for the AEC (ATP + 1/2 ADP)/(ATP + ADP + AMP) are 0.80 or greater in aerobic cells but less than 0.75 in hypoxic cells. Previous studies have shown that under optimal conditions, soybean nodules have AEC values of 0.65 to 0.75 (de Lima et al., 1994; Oresnik and Layzell, 1994), which decrease further by approximately 0.12 when

[1] This research was supported by a Natural Sciences and Engineering Research Council (Canada) research grant to D.B.L., an Australian Research Council grant to C.A.A., and an Alexander von Humboldt Foundation (Germany) grant to H.W.

* Corresponding author; e-mail layzelld@biology.queensu.ca; fax 1–613–545–6617.

Abbreviations: AEC, adenylate energy charge; GDH, glutamate dehydrogenase; HBD, hydroxybutyrate dehydrogenase; Lb, leghemoglobin; PEPC, PEP carboxylase.

nodule metabolism is limited after stem girdling, nitrate fertilization, or exposure to 10% O_2 (de Lima et al., 1994). In contrast, exposure to high O_2 inhibited nitrogenase activity and increased the AEC by approximately 0.11 (de Lima et al., 1994).

To determine the site of hypoxic metabolism, nodules of soybean (*Glycine max*) were frozen rapidly in liquid N_2, ground to a fine powder while frozen, lyophilized, sonicated in nonaqueous solvents, and separated into plant and bacteroid fractions using a nonaqueous density-gradient technique (Gerhardt and Heldt, 1984; Riens et al., 1991) adapted for use with soybean nodules. Under these conditions the distribution of metabolites was not altered during the isolation procedure, a problem inherent in all traditional aqueous methods for organelle separation (Farnden and Robertson, 1980; Reibach et al., 1981). Adenylate concentrations were assessed in the plant and bacteroid compartments of control nodules maintained at an external $[O_2]$ of 21% (v/v) and in nodules inhibited by exposure to 10% O_2 for 3 min.

MATERIALS AND METHODS

Plant Culture

Soybean (*Glycine max* L. Merr. cv Maple Arrow) plants were grown in gas-exchange pots in a plant growth chamber (model PGV36, Conviron, Winnipeg, Manitoba, Canada) as described previously (Kuzma and Layzell, 1994). Plants were inoculated with *Bradyrhizobium japonicum* USDA 16 at planting time and were used for experiments 5 weeks after planting.

Experimental Treatments and Tissue Harvest

Four populations of soybean were used and each was divided into two groups of 15 plants per group. The nodulated roots of the control group were maintained at ambient conditions (21% O_2) before sampling, whereas the nodulated roots of treated plants were switched from 21% O_2 to 10% O_2 in N_2 for 3 min before being frozen and sampled. The 10% O_2 treatment is known to inhibit nitrogenase activity by increasing O_2 limitation (Hunt et al., 1987). Sampling involved rapidly uprooting the nodulated roots from the sand media and immediately plunging them into liquid N_2 (Oresnik and Layzell, 1994). Nodules from all 15 plants within a group were removed from the root system while frozen and ground in liquid N_2 using a mortar and a pestle until a very fine powder was obtained (approximately 1 h). Two subsamples (approximately 0.12 g each) of the homogenized nodule tissue were removed for metabolite and protein analysis, respectively, whereas the remaining tissue was lyophilized for 3 d under a vacuum (−100 kPa) in a flask maintained on an ice/methanol mixture (−15°C) for the first 24 h, then at room temperature for the remaining 2 d. A trap between the sample and the vacuum pump was maintained in liquid N_2 throughout this time. The dried tissue powder was then used for nonaqueous fractionation.

Nonaqueous Fractionation of the Nodule Tissue

A nonaqueous-fractionation method was developed for nodules as a modification of a method designed for leaf tissue (Gerhardt and Heldt, 1984; Riens et al., 1991). The following steps were carried out in a cold room (4°C): Lyophilized nodule tissue (approximately 0.6 g) was sonicated using a microprobe (model 450 sonicator, Branson Ultrasonics, Danbury, CT) in a dry-ice/heptane bath in 25 mL of dry (dried and stored over Molecular Sieve 4A, Fisher Scientific) heptane and tetrachloroethylene mixed at a ratio of 43:57 (v/v) to give 1.23 g mL^{-1} density. The density was checked at 4°C using calibrated hydrometers (Fisher Scientific). Sonication was for 12 min, during which time the material was exposed to four cycles, each including 2 min of 5 s on, 10 s off and 1 min of 15 s off, 2 s on. The sonication step, which was similar to that carried out with leaf tissue in previous nonaqueous studies (Gerhardt and Heldt, 1984; Stitt et al., 1989), was necessary to break the electrostatic and other physical forces that tended to hold the dried 0.3- to 1.0-μ particles together within the nonaqueous solvents. Through sonication a uniform suspension of the dried tissue particles was obtained, thus making it possible to filter the samples and, subsequently, to separate the particles by density-gradient centrifugation.

The sonicated homogenate was filtered through 82-μm nylon mesh to remove any large debris, pelleted by centrifugation at 3000 rpm in a swing-out rotor (clinical centrifuge, International Equipment, Boston, MA) for 10 min, and then resuspended in a dry solvent mixture (density of 1.23 g mL^{-1}) to a final volume of 8.5 mL.

The homogenate was set aside in a closed tube to prevent condensation of water vapor in the solvents, and an exponential density gradient of dry heptane and tetrachloroethylene was prepared using a custom-made glass gradient maker similar to that described previously (Soboll et al., 1979). Thirty milliliters of a 41:59 (v/v) heptane:tetrachloroethylene mixture (density of 1.24 g mL^{-1}) was placed in the open reservoir of the gradient maker; 25 mL of a 25:75 (v/v) mixture of the same solvents (density of 1.4 g mL^{-1}) was placed in the sealed mixing reservoir of the gradient maker. The gradient was created by allowing the contents of the open reservoir to flow through the sealed chamber, which was mixed rapidly using a magnetic stirrer. The gradient was poured into 1- × 3.5-inch nitrocellulose centrifuge tubes (Beckman) containing a 4-mL cushion of pure tetrachloroethylene (density of 1.64 g mL^{-1}). The density of the poured gradient ranged exponentially from 1.29 to 1.4 g mL^{-1}, as shown in Figure 1B. Four milliliters (containing 67.1 ± 3.6 mg of protein) of the homogenate (density of 1.23 g mL^{-1}) was gently placed on top of each gradient and two gradients were run at the same time for each nodule harvest.

The gradients were centrifuged at 12,000 rpm for 2.5 h using a rotor and an ultracentrifuge (models L8–55M and SW28, respectively, Beckman) maintained at 4°C. This resulted in equilibrium distribution of the components in the gradient according to their density. From each gradient, 10 fractions (2–4.5 mL each) were collected, starting at the top and using a single 5-mL glass pipette per gradient to

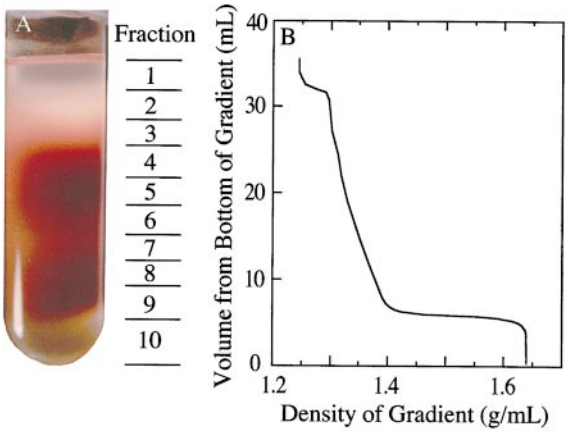

Figure 1. A, Photograph of a nonaqueous (heptane:tetrachloroethylene) gradient of lyophilized particles from soybean nodules. The approximate location of each of the 10 fractions is shown to the right of the photograph. The red color is due to Lb. B, The approximate density of the liquid associated with each fraction of the gradient that is shown in A. The gradient was poured onto a 4-mL cushion of tetrachloroethylene having a density of 1.64 g mL^{-1}, and the sample was loaded in a heptane:tetrachloroethylene mixture having a density of 1.23 g mL^{-1}.

minimize total losses. The approximate locations of these fractions are shown in Figure 1A.

As soon as each fraction was collected, its density was lowered by the addition of approximately 3 to 6 mL of dry heptane before the tissue was pelleted and then resuspended in 1 mL of pure dry heptane. Each fraction was split between two Eppendorf tubes (0.5 mL/tube) containing acid-washed sand. One tube was subsequently used for metabolite analysis and the other for marker enzymes and protein analysis. The subfractions were dried overnight at room temperature under a vacuum (−60 kPa) in a dessiccator with silica gel and candle wax.

Tissue Extraction and Metabolite and Marker Enzyme Analysis

Dried subfraction samples were extracted for metabolites in 1 mL of ice-cold 10% $HClO_4$ containing 2.5 mM EGTA by vortexing each tube for four cycles of 30 s of agitation and 10 s on ice (to cool the samples between each agitation). Resuspended subfractions were left on ice for 15 min before pelleting by centrifugation (14,000 rpm) for 10 min and neutralizing the supernatant with KOH. Adenylates (ATP, ADP, and AMP) were measured in each fraction using enzyme-coupled assays, as described by Oresnik and Layzell (1994).

The second set of dried subfractions was extracted for marker enzyme and protein analysis in 0.5 mL of 0.25 mM phosphate buffer (pH 7.5, containing 0.5 mM EDTA, 0.5 mM DTT, 2 mM PMSF, 15% glycerol [v/v], and 0.1% Triton-X) by vortexing the samples on acid-washed sand, as described for metabolite extraction. Samples were held on ice for 10 min before adding 0.5 mL of a 100 mM phosphate buffer (pH 7.5, containing 0.5 mM EDTA, 0.5 mM DTT, 2 mM PMSF, 15% glycerol [v/v], and 0.1% Triton X-100).

The HBD was assayed as described previously (Farnden and Robertson, 1980) and used as the marker enzyme for bacteroids. Preliminary studies (data not shown) indicated that the distribution of HBD activity among fractions was similar to that of Ala dehydrogenase, another bacterial enzyme (Wiame et al., 1965), and to the reaction of a polyclonal antibody made against the Fe component of *Klebsiella pneumoniae* nitrogenase (Oresnik, 1995). To identify an appropriate marker for the plant compartment, the following enzyme activities of each fraction were assayed on a spectrophotometer (Milton Roy Spectronic 3000, Spectronic Instruments, Rochester, NY) using standard enzyme-coupled assays for PEPC (Gerhardt and Heldt, 1984) and xanthine dehydrogenase (Atkins et al., 1980) as cytosolic markers, and GDH as a mitochondrial marker (Yamaya et al., 1984). In addition, Lb was assayed as a possible cytosolic marker using the pyridine hemochrome method for heme (Appleby and Bergersen, 1980) and an ELISA assay (Engvall and Perlmann, 1971) incorporating antibodies against the soybean Lb apoprotein. The protein content of each fraction was determined using a Bio-Rad protein assay kit.

Determination of Adenylate Contents of the Plant versus Bacteroid Fractions

Because the distribution of marker enzymes was similar in the fractions from the replicate gradients within each of the four nodule populations, the proportions of each adenylate and marker enzyme were averaged from the two gradients for each of the 10 fractions (numbered from the top of the gradient). Therefore, four replicates were available for subsequent calculations of the distribution of adenylates in the bacteroid and plant compartments. These were carried out individually for each of the four replicate gradients.

The proportion of adenylates (to the total nodule content) that could be attributed to the bacteroid and plant compartments of the nodule was determined using a computer program developed by Riens et al. (1991). This program tests all of the possible combinations of metabolite proportions found associated with "marker A" and "marker B" at 1% intervals (i.e. marker A = 1%, marker B = 99% . . . marker A = 99%, marker B = 1%) against experimental data, in this case the proportion of the metabolite distribution to the marker enzymes in all of the fractions. This method assumes that the metabolites and marker enzymes from the same subcellular compartment segregate together into the various fractions of the gradient. The best-fitting metabolite proportions between the bacteroid marker and the plant cell marker with the experimental data, as predicted by the computer program, were used to calculate the metabolite content of the bacteroids and the plant cells' compartment of the nodule.

To calculate the percent recovery of each metabolite, the total recovered from the gradient (in nanomoles per milligram of protein) was divided by the amount (in nanomoles per milligram of protein) of that metabolite measured in the rapidly frozen fresh nodule tissue. To correct for losses during fractionation, the proportion of each metabolite

Table I. *The effect of reducing the rhizosphere [O_2] from air to 10% O_2 (3-min exposure) on the pool sizes of adenylates in rapidly frozen soybean nodules that were subsequently used for nonaqueous fractionation*

Values are presented as means ± SE (n = 4).

Metabolite	Control	10% O_2
	nmol mg^{-1} protein	
ATP	8.3 ± 1.0	7.3 ± 1.1
ADP	5.1 ± 0.6	7.4 ± 1.8
AMP	2.3 ± 0.4	3.8 ± 1.4
Total adenylates	15.7 ± 2.0	18.4 ± 3.8
AEC	0.70 ± 0.009	0.61 ± 0.039

ascribed to the bacteroids or plant cells was multiplied by the total content (in nanomoles per milligram of protein) of the metabolite determined in the frozen nodule tissue that was not lyophilized. This calculation assumes that any losses in metabolites were not differentially associated with either the plant or the bacteroid compartments.

Electron Microscopy of Bacteroid and Plant-Enriched Fractions

Aliquots of fractions 4 and 8 were prepared for electron microscopy by fixing the dried material in aqueous 4% glutaraldehyde and then in 2% osmium tetroxide before dehydration in an acetone series and embedding in Spurr's resin (Spurr, 1969). Sections (0.1 μm) were stained with uranyl acetate and lead citrate and the electron micrographs were obtained using a transmission electron microscope (model JEM 2000FXII, Jeol). Although rehydration of the material in the glutaraldehyde solution may have modified disrupted membranes, it was found to be necessary. In preliminary studies fixing and substituting the dry material directly in 2% osmium tetroxide in pure acetone at −80°C resulted in most of the material falling out of the thin sections (data not shown).

RESULTS

Metabolite Content and AEC of Whole Nodules under Ambient and Low O_2

In rapidly frozen soybean nodules assayed directly for adenylates, no significant differences were measured in adenylate pools between nodules from plants maintained in air (control plants) and those in which the nodulated roots were exposed to 10% O_2 for 3 min (treated plants) (Table I). However, mean AEC values calculated from individual samples were significantly different, being greater in the control (0.70 ± 0.01) than in the treated (0.61 ± 0.04) nodules (Table 1).

Identification of Marker Enzymes

When the frozen tissue had been ground, lyophilized, sonicated, and fractionated on a nonaqueous gradient, the resultant profile showed distinct bands or zones of red- and white-colored material (Fig. 1). The gradients were separated into 10 fractions, as shown in Figure 1, and aliquots of each were taken for analysis of potential marker enzymes. Initially, HBD, Ala dehydrogenase, and the Fe protein of nitrogenase were assayed as potential markers for bacteroids. HBD was chosen because its separation was similar to that of the other enzymes (data not shown), its activity was relatively high, and the assay was simple.

A number of potential markers for the plant compartments were also examined. All of these fractionated differently from HBD (Fig. 2), providing evidence that the gradient was able to separate plant- and bacterial-enriched fractions. As a cytosolic marker, PEPC was determined to be better than the heme of Lb, because the heme of Lb and the apoprotein of Lb fractionated differently from one another (Fig. 2A). Proportionately, more of the heme of Lb than the apoprotein of Lb was associated with HBD, suggesting that a small but significant amount of the heme in the nodule may be in bacteroids, compromising the assumption that the heme of Lb marked the plant cytosol fraction. The apoprotein of Lb distribution resembled that of PEPC.

PEPC fractionated in much the same way as xanthine dehydrogenase (Fig. 2A) and GDH (Fig. 2B), showing that the nonaqueous gradient could distinguish between bacteroid- and plant-enriched fractions, but could not separate the plant subcellular components. Therefore, we used PEPC as the marker enzyme for the entire plant fraction. Previous studies (Robinson et al., 1996) have shown that PEPC is present in the cytosol of both infected and noninfected cells, as well as cortical cells, although to a lesser degree.

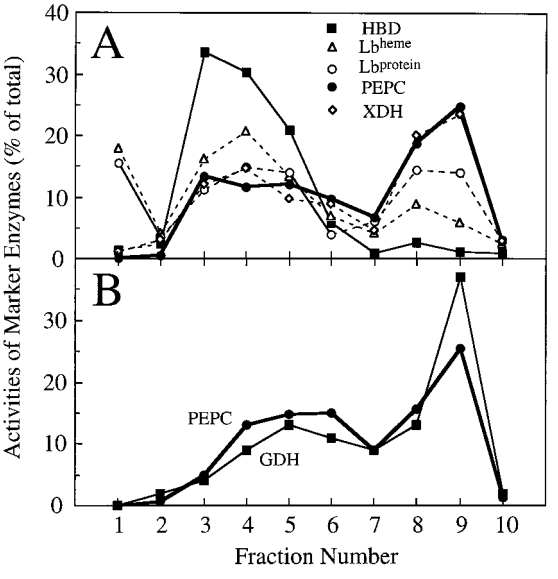

Figure 2. The distribution of potential marker enzymes or proteins for bacteroid or plant cell compartments obtained in each of the 10 fractions that comprised a nonaqueous gradient of lyophilized nodule tissue. A, A gradient in which assays were carried out for HBD, the heme group of Lb (Lb^{heme}), the apoprotein of Lb ($Lb^{protein}$), PEPC, and xanthine dehydrogenase (XDH). B, A gradient in which assays were carried out for PEPC and GDH.

Recovery of Marker Enzymes and Metabolites from the Nonaqueous Gradients

The recoveries of marker enzymes and adenylates from the nonaqueous gradients were expressed as a percentage of the amount measured directly in extracts from the rapidly frozen nodules (Table II). The HBD activity recovered from the gradient was 154% (treatment) and 220% (control) of that in fresh nodule tissue, indicating that the lyophilization, sonication, and exposure to nonaqueous solvents were able to elicit greater HBD activity than a simple aqueous buffer extraction of fresh tissue. This finding is consistent with the observation that maximum HBD activity from fresh tissue required two or more passages through a French press at 16,000 p.s.i. units (Oresnik, 1995). All other marker enzymes and metabolites that were assayed showed recoveries that varied from 85% to 129% of that measured in the fresh tissue, and no mean values were significantly different from 100% (Table II).

Distribution of Marker Enzymes and Adenylates within the Gradients

The distribution of HBD, PEPC, and protein was very similar in the gradient fractions that were used to separate the lyophilized particulate components from the four control and in the four treated populations of the nodules (Fig. 3). The HBD activity was highest in fraction 4 (Fig. 3A), whereas PEPC activity peaked in fractions 8 and 9, with a lesser peak in fraction 4 (Fig. 3B). These activities correlated with the regions of intense red color in the gradients, although a large amount of HBD activity was associated with white-colored particulate material in fraction 3 (Fig. 1A).

No significant differences were observed in the proportional distribution of HBD activity between the control and treatment gradients (Fig. 3A). Similarly, PEPC and total protein distribution were not significantly different between treatments, except for the protein fraction 7 (Fig. 3, B and C). These results were in contrast to those for the proportional distribution of adenylates, where significant differences were observed between control and treated nodules in a number of fractions, particularly nos. 3, 5, 6, and 7 (Fig. 4). Although these differences were subtle, they demonstrated that the 10% O_2 treatment altered the adenylate pools in the nodule.

Table II. *Recovery of marker enzyme activity and adenylates from the nonaqueous gradients from the same population of plants*

Values are presented as means ± SE (n = 4).

Marker Enzyme or Metabolite	Recovery from Nonaqueous Gradients	
	Control	10% O_2
	% of that measured in frozen, fresh nodule tissue	
Marker enzymes		
HBD	220 ± 51	154 ± 54
PEPC	94 ± 12	107 ± 11
Metabolites		
ATP	93 ± 6	96 ± 8
ADP	129 ± 20	104 ± 21
AMP	85 ± 16	79 ± 25
Total adenylates	119 ± 11	93 ± 16

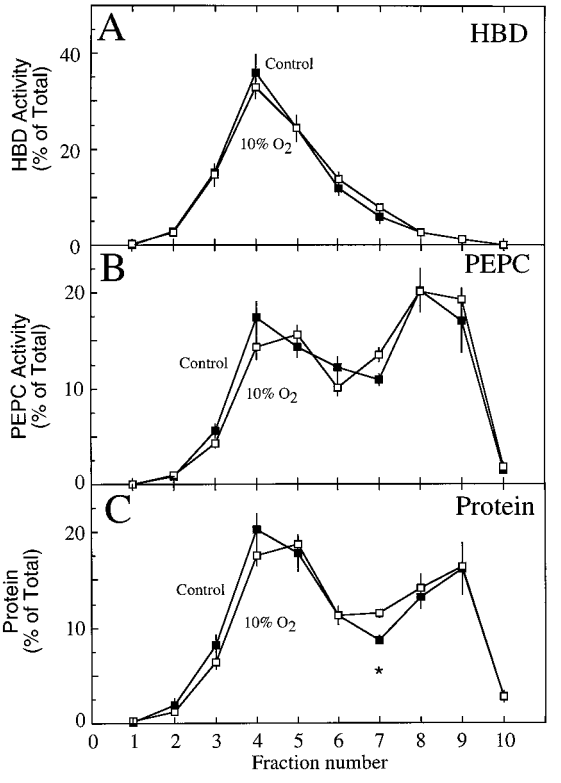

Figure 3. The proportional distribution of HBD (A), PEPC (B), and protein (C) within the fractions taken from a nonaqeuous gradient of lyophilized particles from soybean nodules of control plants (■) and of nodulated roots exposed to 10% O_2 for 3 min (□). Values are presented as the mean (±SE) of four replicates, each replicate being the mean of two gradients that were run simultaneously on nodule material harvested from a single population of plants. Values within a fraction that were significantly different ($P = 0.05$) between control and treated nodules are marked with an asterisk.

Electron Microscopy of the Gradient Fractions

Electron micrographs of the nonaqueous fraction that was enriched in HBD (Fig. 5A) clearly showed the presence of many bacteroids interspersed with amorphous material. In contrast, micrographs of the plant-enriched fraction (Fig. 5B) showed few bacteroids and appeared to contain large amounts of amorphous material (presumably cytosol) and portions of organelles (presumably mitochondria and plastid membranes). The bacteroids were better able to maintain their structure than the plant organelles in spite of the stresses to which the tissues were exposed during the nonaqueous fractionation and preparation for microscopy.

Adenylates and AEC in Plant and Bacteroids under Ambient and Low-O_2 Treatment

To obtain an estimate of how much of each metabolite was associated with the bacteroid compared with the plant compartment, the proportional distribution of the marker

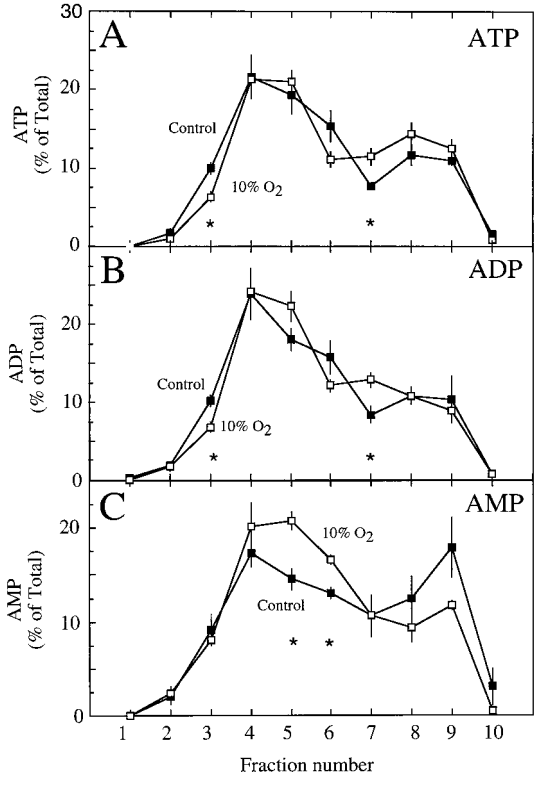

Figure 4. The proportional distribution of ATP (A), ADP (B), and AMP (C) within the fractions taken from a nonaqeuous gradient of lyophilized particles from soybean nodules of control plants (■) and from nodules of nodulated roots exposed to 10% O_2 for 3 min (□). Values are presented as the mean (±SE) of four replicates. Values within a fraction that were significantly different (P = 0.05) between control and treated nodules are marked with asterisks.

enzymes and metabolites from gradients associated with individual plant populations were entered into the computer program of Riens et al. (1991). The plant compartment was estimated to contain 63% ± 3% and 56% ± 2% of the total adenylates in the control group and in those treated with 10% O_2, respectively. These values were not significantly different (P = 0.05) from one another and were similar to those obtained in an earlier study (Oresnik and Layzell, 1994) that used an aqueous-fractionation technique to quantify the distribution of total adenylates in fractions from soybean nodules.

The ATP, ADP, and AMP pool sizes calculated to exist in the bacteroid and plant fractions are shown in Figure 6, A and B, respectively. Due to the large variance, no significant differences were observed in any of the pool sizes between control and treated plants. However, when AEC values were calculated for plant and bacteroid compartments from each of the four nodule populations, the AEC in bacteroids was found to be significantly lower (P = 0.05) in the treated (0.56 ± 0.06) than in the control (0.76 ± 0.05) nodules (Fig. 5C). In contrast, the AEC in the plant fraction was not affected by the treatment and remained at 0.65 ± 0.02. Therefore, in whole control nodules, the relatively low AEC (0.70 ± 0.01) was a composite of a high bacteroid AEC and a low plant AEC. The decrease in whole-nodule AEC that occurred when nodules were exposed to 10% O_2 (Table I) was associated with a reduction in the AEC of the bacteroid, not of the plant component of the nodule.

DISCUSSION

The Nonaqueous Separation of Nodule Fractions

This study is the first report, to our knowledge, of the nonaqueous fractionation of nodule tissue into its component parts to identify in vivo pool sizes of key metabolites. By maintaining the vacuum flask containing nodule tissue in an ice/methanol mixture (−15°C) for the first 24 h of lyophilization, and by allowing a full 3 d for lyophilization while maintaining a liquid N_2 trap in the vacuum line, it was possible to avoid the large (about 60%) losses in the adenylate pools that occurred in previous studies (Oresnik and Layzell, 1994). High recoveries were also obtained for the marker enzyme PEPC (Table I). The abnormally high (154%–220%) recovery for HBD was attributed to the fact that high pressure is required to extract full HBD activity from fresh bacteroids (Oresnik, 1995). Presumably, sonication of the lyophilized tissue extracted a larger proportion of the enzyme activity than the simple aqueous-buffer extraction of fresh, frozen nodules. Assuming that there were no treatment effects on the ability of sonication to extract HBD activity from bacteroids, the high percentage of recovery should have no effects on the findings of this study.

Unlike aqueous-gradient fractionation of legume nodules (Farnden and Robertson, 1980; Reibach et al., 1981), in which bacteroids are more dense than most plant organelles, in the nonaqueous gradients developed here, the bacteroid fractions were localized near the top of the gradient and the plant fraction was recovered near the bottom. This was confirmed not only by electron microscopy (Fig. 5), but by HBD activity (Fig. 3A), Ala dehydrogenase activity, and localization of the Fe protein of nitrogenase (data not shown). Presumably, grinding, lyophilization, and sonication of frozen nodules resulted in dried plant material that was more dense than that of the bacteroids.

The method described here achieved highly enriched plant fractions (fractions 8 and 9) with little contamination from bacteroids, but was less successful in achieving bacteroid-enriched fractions (fractions 4–6) that were free of plant material. This would be expected if some dried symbiosome membranes and cytosolic material remained attached to the bacteroids during fractionation. The fact that the cytosolic apoprotein Lb marker (representing infected cells only) was proportionately higher in the bacteroid-enriched fractions and lower in the plant-enriched fractions than the cytosolic PEPC marker (representing infected and noninfected cells) is consistent with this proposition. Nevertheless, the separation that was achieved was sufficient for the computer program to attribute reliably each adenylate to the two cell compartments.

AEC and O_2 Limitation in Control Nodules

The observation that active, control nodules of soybean had AEC levels (0.70 ± 0.009; Table I) typical of hypoxic or

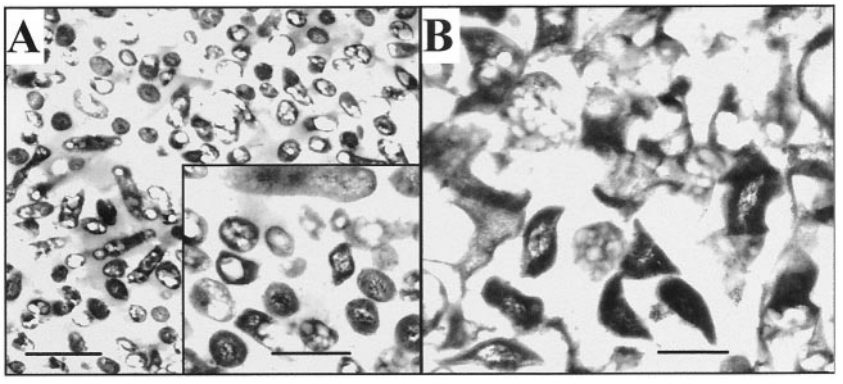

Figure 5. Electron micrographs of the nodule material from fractions 4 (A) and 8 (B) of the nonaqueous gradient. Fraction 4 was dominated by bacteroids, whereas in the material from fraction 8, it was difficult to distinguish any particular cellular structures. Bars = 2 μm (A) and 0.5 μm (inset and B).

anaerobic tissues (Pradet and Raymond, 1983) confirmed previous findings (de Lima et al., 1994; Oresnik and Layzell, 1994). Typically, fully aerobic tissues have AEC values that are 0.80 or greater (Pradet and Raymond, 1983). The low AEC in legume nodules has been provided as further evidence that their respiration and nitrogenase activity is limited by the availability of O_2 (Hunt and Layzell, 1993).

Through nonaqueous fractionation, the low AEC of control nodules was attributed primarily to the plant compartment (AEC = 0.65 ± 0.04), whereas the bacteroid compartment had an AEC (0.76 ± 0.05) that was close to that found in fully aerobic organisms. Because the nodule cortex contains less than 5% of the adenylates in whole nodules (Oresnik and Layzell, 1994), and because 72% to 90% of the central zone tissue is occupied by infected cells (Lin et al., 1988; Dakora and Atkins, 1990), the adenylate pools measured in this study probably reflected conditions in the bacteria-infected cells.

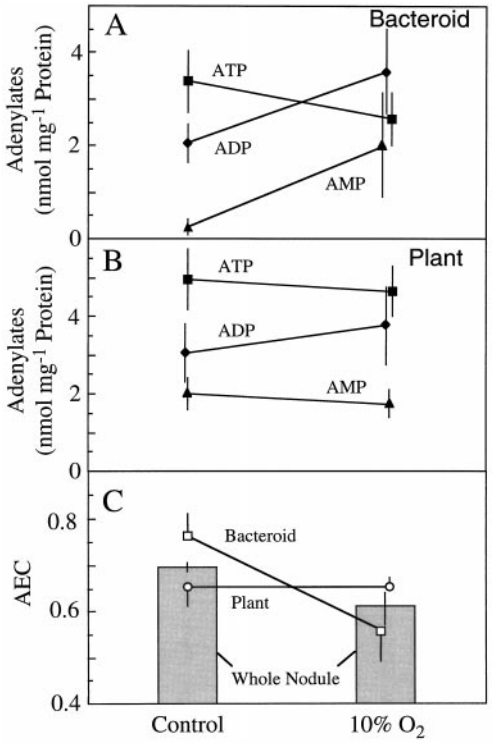

Figure 6. The effect of exposing nodulated soybean roots to 10% O_2 for 3 min on the pool sizes of ATP (■), ADP (◆), and AMP (▲) in the bacteroid (A) and plant (B) compartments of soybean nodules. These values were used to calculate the AEC ([ATP + 0.5 ADP]/[ATP + ADP + AMP]) (C) for the bacteroid (□) and plant (○) compartment of nodules and for whole nodules ▨. Values are presented as the means (±SE) of four replicates, each of which is the mean of two gradients that were run simultaneously using nodule material harvested from a single population of plants.

These findings are consistent with the observation that the terminal oxidases in bacteroids have a higher affinity to O_2 (5–26 nM; Bergerson and Turner, 1990, 1993) than those in nodule mitochondria (50–100 nM; Rawsthorne and LaRue, 1986; Millar et al., 1995). Thus, the relatively low [O_2] found within the infected cells (<60 nM; Kuzma et al., 1993) may be sufficient for bacteroid metabolism but limiting for mitochondrial metabolism.

A major problem with this interpretation is the cytological evidence that mitochondria are clustered around the gas-filled intercellular spaces within the infected tissue zone of the nodule (Millar et al., 1995), and mathematical models that predict large free-O_2 gradients in this region of the cell (Bergersen, 1994; Thumfort et al., 1994). Therefore, the mitochondria within the infected cell may occupy a very different microenvironment (100 to >1000 nM O_2) than the bacteroids (3–40 nM O_2) with respect to O_2 availability. If this is the case, it is difficult to see how mitochondrial metabolism could be O_2 limited.

Adenylate Energy Charge and O_2 Limitation in Nodules Inhibited by 10% O_2

If an O_2 limitation within the plant fraction is responsible for the low (i.e. <0.80) AEC in active, N_2-fixing nodules, then imposing a more severe O_2 limitation on the nodule should further reduce the AEC of the plant fraction. This was not observed in the present study. Three minutes of exposure to 10% O_2 causes a rapid inhibition of nitrogenase activity and nodule respiration (Hunt et al., 1987), a sharp reduction in infected cell [O_2] (King et al., 1988; Layzell et al., 1990), and a decrease in the AEC of the whole nodule (Table I) (de Lima et al., 1994). However, the AEC of the plant fraction was unaffected by the 10% O_2 treatment, whereas the AEC of bacteroids declined sharply from 0.76 to 0.56 (Fig. 6).

These findings suggest that it is the bacteroids, not the plant compartment of the nodule, that is the primary site of O_2-limited metabolism.

Adenylates and the Site of O_2 Limitation in Soybean Nodules

Low AEC values in plant tissues occur when the rate of ATP synthesis does not keep up with the rate of ATP utilization. This may or may not be due to an O_2 limitation of nodule metabolism.

For example, it is possible that the 10% O_2 treatment decreased ATP demand within the plant compartment, thereby offsetting any O_2 limitation on mitochondrial activity and accounting for the lack of a change in plant AEC. In the infected cells the most important sink for ATP would be Gln synthetase, an enzyme responsible for assimilating the NH_4^+ produced by nitrogenase. Because nitrogenase activity would be inhibited by the 10% O_2 treatment, the ATP demands of Gln synthetase would decline with time. However, this is not likely to account for the results of the present study, because the pools of NH_4^+ are large in nodules and are probably not depleted during the 3-min exposure to 10% O_2. Support for this conclusion comes from studies (King, 1989; Walsh et al., 1989) that have examined pool sizes of NH_4^+, amino acids, and ureides in nodules following exposure to Ar:O_2, a treatment that stops NH_4^+ production and is therefore more severe than the 50% reduction in NH_4^+ production associated with 10% O_2 exposure. Following Ar:O_2 treatment, nodule NH_4^+ and amino acid pools were still approximately 70% of their initial levels after 60 min (King, 1989), and ureide pools were maintained for 20 to 30 min (King, 1989) before they declined, with a half-time of about 2 h (Walsh et al., 1989). It seems unlikely that there would be a significant reduction in the plant's demand for ATP in NH_4^+ assimilation during the initial 3 min of exposure to 10% O_2.

The simplest explanation for the lack of a 10% O_2 effect on plant AEC is that the plant fraction is not a site of O_2-limited metabolism in nodules. If this is the case, why was the plant AEC so low (0.65) and typical of that found in tissues having hypoxic metabolism? This could be explained as a characteristic of the infected cells. Bacteria-infected cells are much larger (having radii of approximately 30 μm) than most other plant cells (having radii of approximately 5–10 μm). The sinks for ATP within the plant compartment (e.g. symbiosome ATPases or Gln synthetase) would occur throughout the entire cell, in many cases at long distances from the mitochondria that are clustered near the gas-filled spaces. The translocation of ATP from the mitochondria to extra mitochondrial sites within the cell and the translocation of ADP and AMP back to and into the mitochondria may be the major factor limiting the rate of ATP synthesis in these cells. This proposal may explain why the 10% O_2 treatment did not affect the AEC of the plant fraction. It would help to resolve an apparent discrepancy between the results of the present study and those of mathematical models that have predicted that the mitochondria may be in a microenvironment where [O_2] greatly exceeds the K_m (O_2) of the terminal oxidase (Bergersen, 1994; Thumfort et al., 1994).

When the [O_2] around the nodule was decreased to 10%, the sharp decline in the AEC of the bacteroid fraction was most readily explained as an O_2 limitation of ATP synthesis. This treatment results in inhibition of nitrogenase activity to 30% of initial values within 2 to 3 min (Hunt et al., 1987; de Lima et al., 1994), and a corresponding decline in the AEC of the whole nodule (de Lima et al., 1994), as shown in Table I.

Researchers have long assumed that bacteroids were the site of O_2-limited metabolism in legume nodules (Bergersen, 1962, 1984; Dilworth, 1974; McDermott et al., 1989; Werner, 1992). However, to our knowledge, this study is the first to provide evidence that illustrates this in intact, attached nodules. Although the mechanism of nitrogenase inhibition is unknown, it could be attributed to a shortage of ATP in meeting the metabolic needs of nitrogenase or to a direct inhibition of the nitrogenase enzyme by ADP (Miller et al., 1986).

Nonaqueous Fractionation and the Study of Nodule Metabolism

The nonaqueous method described here is potentially a powerful tool for the study of C and N metabolism in legume nodules. In addition to its use in studies of adenylates, it could monitor changes in the pool sizes of metabolites such as malate, PEP, pyruvate, or Gln, after perturbations in O_2 supply, carbohydrate availability, or N fixation, and thereby provide insight into the factors that regulate subcellular pools of metabolites.

Preliminary studies indicate that it may be possible (with some modifications to the gradient) to obtain fractions that are enriched in individual organelles such as mitochondria and plastids. For example, if separate mitochondrial and cytosolic fractions could be recovered, it may be possible to test the hypothesis proposed here, that the mitochondria are fully aerobic in nodules and that the low AEC in the plant compartment is a result of the long diffusion path from the mitochondria to the site of ATP utilization.

ACKNOWLEDGMENTS

We would like to thank Drs. Cyril Appleby and David Goodchild for their gift of antibodies to soybean Lb apoprotein, Drs. David Day and Fraser Bergersen for useful criticisms of the manuscript, Robert Campbell for construction of the gradient maker, Dr. Stephen Hunt for photographing the gradient, and Natalie Fletcher for assistance with the electron microscopy.

Received September 15, 1998; accepted October 23, 1998.

LITERATURE CITED

Appleby CA, Bergersen FJ (1980) Preparation and use of Lb for evaluating biological nitrogen fixation. *In* FJ Bergersen, ed, Methods for Evaluating Biological Nitrogen Fixation. John Wiley & Sons, New York, pp 315–333

Atkins CA, Rainbird R, Pate JS (1980) Evidence for a purine pathway of ureide synthesis in nitrogen-fixing nodules of cowpea (*Vigna unguiculata* (L) Walp). Z Pflanzenphysiol **97:** 249–260

Bergersen FJ (1962) The effects of partial pressure of oxygen upon respiration and nitrogen fixation by soybean root nodules. J Gen Microbiol **29:** 113–125

Bergersen FJ (1984) Oxygen and the physiology of diazotrophic microorganisms. *In* C Weeger, WE Newton, eds, Advances in Nitrogen Fixation Research. Martinus Nijhoff/Dr. W. Junk, The Hague, The Netherlands, pp 171–181

Bergersen FJ (1994) Distribution of O_2 within infected cells of soybean root nodules: a new simulation. Protoplasma **183:** 49–61

Bergersen FJ, Turner GL (1990) Bacteroids from soybean root nodules: respiration and N_2 fixation in flow-chamber reactions with oxyleghaemoglobin. Proc R Soc London **238:** 295–320

Bergersen FJ, Turner GL (1993) Effects of concentration of substrates supplied to N_2 fixing soybean bacteroids in flow chamber reaction. Proc R Soc London Ser B **251:** 103–109

Ching TM, Bergersen FJ, Turner GL (1981) Energy status, growth and nitrogenase activity in continuous cultures of *Rhizobium* sp. strain CB756 supplied with NH_4^+ and various rates of aeration. Biochim Biophys Acta **636:** 82–90

Dakora FD, Atkins CA (1990) Morphological and structural adaptation of nodules of cowpea to functioning under sub- and supra-ambient oxygen pressure. Planta **182:** 572–582

de Lima M, Oresnik IJ, Fernando SM, Hunt S, Smith R, Turpin DH, Layzell DB (1994) The relationship between nodule adenylates and the regulation of nitrogenase activity by oxygen in soybean. Physiol Plant **91:** 687–695

Denison RF, Hunt S, Layzell DB (1992) Nitrogenase activity, nodule respiration and O_2 permeability following detopping of alfalfa and birdsfoot trefoil. Plant Physiol **98:** 894–900

Dilworth MJ (1974) Dinitrogen fixation. Annu Rev Plant Physiol **22:** 121–140

Engvall E, Perlmann P (1971) Enzyme-linked immunosorbent assay (Elisa) quantitative assay of immunoglobulin G. Immunochemistry **8:** 871–874

Farnden KJF, Robertson JG (1980) Methods for studying enzymes involved in metabolism related to nitrogenase. *In* FJ Bergersen, ed, Methods for Evaluating Biological Nitrogen Fixation. John Wiley & Sons, New York, pp 265–314

Gerhardt R, Heldt HW (1984) Measurement of subcellular metabolite levels in leaves by fractionation of freeze-stopped material in nonaqueous media. Plant Physiol **75:** 542–547

Hartwig U, Boller B, Nosberger J (1987) Oxygen supply limits nitrogenase activity of clover nodules after defoliation. Ann Bot **59:** 285–291

Hunt S, King BJ, Canvin DT, Layzell DB (1987) Steady and non-steady gas exchange characteristics of soybean nodules in relation to the oxygen diffusion barrier. Plant Physiol **84:** 164–172

Hunt S, King BJ, Layzell DB (1989) Effects of gradual increases in oxygen on nodule activity in soybean. Plant Physiol **91:** 315–321

Hunt S, Layzell DB (1993) Gas exchange of legume nodules and the regulation of nitrogenase activity. Annu Rev Plant Physiol Plant Mol Biol **44:** 483–511

King BJ (1989) Regulation of the diffusion barrier in root nodules of soybean. PhD thesis, Queen's University, Kingston, Ontario, Canada

King BJ, Hunt S, Weagle GE, Walsh KB, Pottier RH (1988) Regulation of O_2 concentration in soybean nodules observed by in situ spectroscopic measurement of Lb oxygenation. Plant Physiol **87:** 296–299

King BJ, Layzell DB (1991) Effect of increases in O_2 concentration during the argon-induced decline in nitrogenase activity in root nodules of soybean. Plant Physiol **96:** 376–381

Kuzma MM, Hunt S, Layzell DB (1993) Role of oxygen in the limitation and inhibition of nitrogenase activity and respiration rate in individual soybean nodules. Plant Physiol **101:** 161–169

Kuzma MM, Layzell DB (1994) Acclimation of soybean nodules to changes in temperature. Plant Physiol **106:** 263–270

Layzell DB, Hunt S, Palmer GR (1990) Mechanism of nitrogenase inhibition in soybean nodules. Pulse-modulated spectroscopy indicates that nitrogenase activity is limited by O_2. Plant Physiol **92:** 1101–1107

Lin JJ, Walsh KB, Canvin DT, Layzell DB (1988) Structural and physiological basis for effectivity of soybean nodules formed by fast-growing and slow-growing bacteria. Can J Bot **66:** 526–534

McDermott TR, Griffith SM, Heichel GH, Vance CP, Graham PH (1989) Carbon metabolism in *Bradyrhizobium japonicum* bacteroids. FEMS Microbiol Rev **63:** 327–340

Millar AH, Day DA, Bergersen FJ (1995) Microaerobic respiration and oxidative phosphorylation by soybean nodule mitochondria: implications for nitrogen fixation. Plant Cell Environ **18:** 715–726

Miller RW, Al-Jobore A, Berndt WB (1986) Properties of alfalfa-*Rhizobium meliloti* symbiotic nitrogenase enzyme system *in vivo* and *in vitro*. Biochem Cell Biol **64:** 556–564

Oresnik IJ, Layzell DB (1994) Composition and distribution of adenylates in soybean nodule tissue. Plant Physiol **104:** 217–225

Oresnik IJ (1995) A biochemical basis for oxygen limitation in legume nodules. PhD thesis, Queen's University, Kingston, Ontario, Canada

Pradet A, Raymond P (1983) Adenine nucleotide ratios and adenylate energy charge in energy metabolism. Annu Rev Plant Physiol **34:** 199–224

Privalle LS, Burris RH (1983) Adenine nucleotide levels in and nitrogen fixation by the cyanobacterium *Anabaena* sp. strain 7120. J Bacteriol **154:** 351–355

Rawsthorne S, LaRue TA (1986) Preparation and properties of mitochondria from cowpea nodules. Plant Physiol **81:** 1092–1096

Reibach PH, Mask PL, Streeter JG (1981) A rapid one-step method for the isolation of bacteroids from root nodules of soybean plants, utilizing self-generating Percoll gradients. Can J Microbiol **27:** 491–495

Riens B, Lohaus G, Heineke D, Heldt HW (1991) Amino acid and sucrose content determined in the cytosolic, chloroplastic, and vacuolar compartments and in the phloem sap of spinach leaves. Plant Physiol **97:** 227–233

Robinson DL, Pathirana SM, Gantt JS, Vance CP (1996) Immunogold localization of nodule-enhanced phosphoenolpyruvate carboxylase in alfalfa. Plant Cell Environ **19:** 602–608

Soboll S, Elbers R, Heldt HW (1979) Metabolite measurements in mitochondria and in the extramitochondrial compartments by fractionation of freeze-stopped liver tissue in nonaqueous media. Methods Enzymol **56:** 201–221

Spurr AR (1969) A low viscosity epoxy resin embedding medium for electron microscopy. J Ultrastruct Res **26:** 31–34

Stitt M, Lilley RM, Gerhardt R, Heldt HW (1989) Metabolite levels in specific cells and subcellular compartments of plant leaves. Methods Enzymol **174:** 518–552

Thumfort PP, Atkins CA, Layzell DB (1994) Re-evaluation of the role of the infected cell in the control of oxygen diffusion in legume nodules. Plant Physiol **105:** 1321–1333

Upchurch RG, Mortenson LE (1980) In vivo energetics and control of nitrogen fixation: changes in the adenylate energy charge and ADP/ATP ratio of cells during growth on dinitrogen versus growth on ammonia. J Bacteriol **143:** 274–284

Vessey JK, Walsh KB, Layzell DB (1988) Oxygen limitation of nitrogen fixation in stem-girdled and nitrate-treated soybean. Physiol Plant **73:** 113–121

Walsh KB, Canny MJ, Layzell DB (1989) Vascular transport and soybean nodule function: II. A role for phloem supply in product export. Plant Cell Environ **12:** 713–723

Werner D (1992) Physiology of nitrogen fixing legume nodules: compartments and functions. *In* G Stacey, RH Burris, HJ Evans, eds, Biological Nitrogen Fixation. Chapman and Hall, New York, pp 391–431

Wiame JM, Pierard A, Ramos F (1965) L-alanine dehydrogenase from *Bacillus subtilus*. Methods Enzymol **5:** 673–675

Witty JF, Minchin FR, Scot L, Revsbech NP (1987) Direct evidence for changes in the resistance of legume root nodules to O_2 diffusion. J Exp Bot **38:** 1129–1140

Yamaya T, Oaks A, Matsumoto H (1984) Characteristics of glutamate dehydrogenase in mitochondria prepared from corn shoots. Plant Physiol **76:** 1009–1013